Magnetic modeling of radial-flux and axial-flux permanent-magnet motors for direct drive automotive

Specifications and comparison

Romain-Bernard Mignot, Didier Chamagne, Frédéric Dubas, Christophe Espanet

ENERGY Department, University of Franche-Comté (UFC)
FEMTO-ST Institute (UMR CNRS 6174), Belfort, France

ABSTRACT. *This paper presents an innovative motorization, i.e., an axial-flux permanent-magnet (PM) motor (AFPMM), for direct drive automotive, mainly for electric vehicles (EVs). The AFPMM has been designed from a three-dimensional (3-D) finite-element analysis (FEA). To demonstrate these electromechanical performances, this motorization has been compared to a radial-flux PM motor (RFPMM) having the same outer diameter and the same rotor polarity. The RFPMM has been simulated by using a two-dimensional (2-D) FEA. The optimization procedure is based on a multi-parametric approach with FEA. Comparison of the results between the two electrical machines has been presented supporting the conclusion that this AFPMM will provide interesting industrial perspectives.*

RÉSUMÉ. *Le présent sujet étudie la faisabilité électromécanique et technico-industrielle d'une nouvelle conception de machine à flux axial dans le but de pouvoir se positionner sur le marché concurrentiel de la traction automobile légère. L'originalité de cette nouvelle motorisation est due à la conception de son stator en « U » et de son rotor à aimants étagés ainsi que de sa connectique d'alimentation des différents bobineaux. Afin de démontrer ses performances électromécaniques, cette nouvelle machine à flux axial est comparée à une motorisation synchrone classique à aimants permanents montés en surface faisant office de référence, ayant le même diamètre extérieur et la même polarité rotorique. La modélisation électromagnétique de chaque machine est réalisée grâce à un modèle numérique par éléments finis en 3D et optimisée par logiciel utilisant les plans d'expériences. Un comparatif détaillé des résultats est présenté. Ce dernier permet de conclure que la motorisation à flux axial nouvellement conçue augure de perspectives industrielles intéressantes.*

KEYWORDS: *direct drive automotive, finite-element analysis, optimization, permanent-magnet, synchronous machine.*

MOTS-CLÉS: *machine synchrone à flux radial, machine synchrone à flux axial, modélisation par éléments finis 3D, optimisation par plans d'expériences.*

1. Introduction

This paper aims at assessing the potential of an axial flux PM machine for direct drive automotive, mainly for electric vehicles (EVs).

In integrated systems, an important requirement is to select the most suitable electrical machine for a particular application. Traditionally, it has been used almost exclusively machines of the radial-flux type. If the machine axial length is limited by the application demands, the electrical machine based on the axial-flux topology may be a competitive or even a better choice.

It is the industry's interest to build reliable, high-performance electrical machines at the lowest cost possible. Constraints that restrict the business are the efficiency, cooling and mechanical properties of the machines. If industry is offered an opportunity to choose between two alternative electrical machines, which have the same performance, e.g. efficiency, but of which one can be built at a lower manufacturing cost, it is obvious that the latter, cheaper design will be preferred. An important tool needed for decision-making is then a performance comparison between the considered electrical machines.

This study focuses on axial-flux machines with one rotor – two stators configuration. This particular axial-flux machine configuration proves to be the most adequate structure for the considered low-speed high-torque industrial applications. The reason is that, firstly, fixing of the stators may be arranged reasonably easily. Secondly, an axial loading of bearings is small due to the internal rotor configuration.

In this paper, we have chosen to use an AFPMM, since this type of machine has a high potential specific torque. It's a motorization physical structure that fits with the expectations of previous industrial constraints. Moreover, the motor sizing should also be small enough short but very accurate, so that the use of a numerical model with an optimization procedure is preferred to an approach with an analytical model. The latter should be rather used in a second step of the design.

To demonstrate its electromechanical performance, this motorization is compared with a RFPMM having the same outer diameter and the same rotor polarity. A detailed comparison of the results is presented further. It is concluded that this AFPMM will provide interesting industrial perspectives.

2. Technical specifications

2.1. Speed/Torque performance and geometric objectives

A direct drive (see Figure 1) with one electric motor per front wheel is chosen to limit the mechanical parts and also to gain space in the vehicle. Table 1 summarizes the characteristics of the electric vehicle that is used. The maximal speed of the

electric vehicle, in which the machine must be installed, is 110 km/h. The European regulations require that the mechanical power of "quadricycles" be limited to 15 kW (NRCQL, 2002).

Figure 1. Citizen_Citi Technologie Prototypes

Table 1. Technical Characteristics

$V_{vehicle}$: 110 km/h	Tire: 135/70-R15	Battery voltage: 350 V
γ : 0 at 50 km/h in 13 sec	C_x : 0.35	$m_{vehicle}$: 850 kg
Slope at 50 km/h : 11 %	$S_{frontal}$: 1.8 m²	$K_{bearing}$: 0.01

In order to verify that the vehicle characteristics (see Table 1) do not impose the use of an electric motor with a mechanical power greater than 15 kW, an analytical model representing Vehicle Dynamics was established (Wurtz, 2005) and submitted to the American Federal Urban Driving Schedule (FUDS) cycle (see Figure 2) (FTPR, 1996).

Indeed, it is this cycle that is most used to evaluate the consumption of electric vehicle batteries (Kroeze, Philipp, 2011). The FUDS cycle coupled to the vehicle technical specifications require that a set of operating points (*i.e.,* torque and mechanical power) must be performed by the vehicle electric motors.

These operating points are shown in Figure 3 and 4. The results show that the electric motor in these specific conditions complies with the regulations governing quadricycles. Other speed cycles (U.S_EPA, 2010) like the urban Federal Test Procedure (FTP) or the Dynamic Urban Driving Schedule (DUDS) were tested. The results confirmed those obtained with the FUDS cycle.
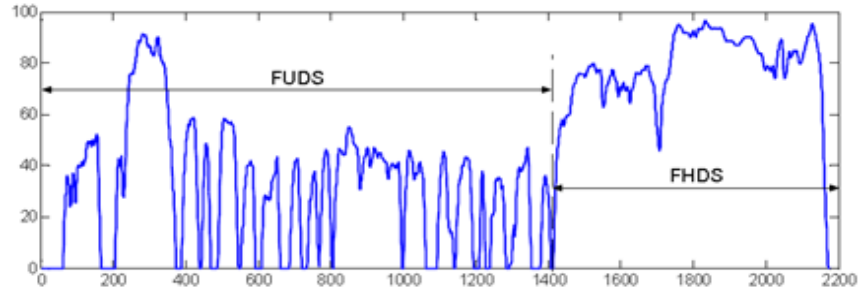
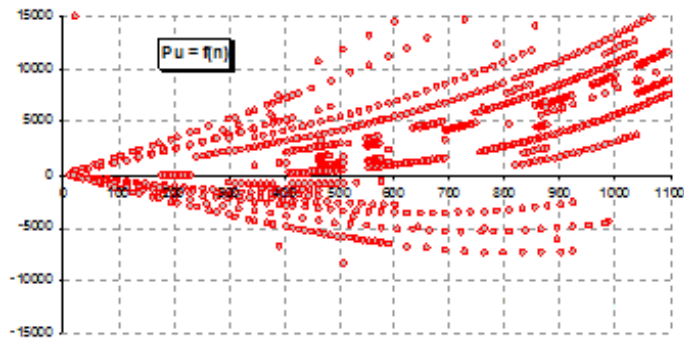*Figure 2. Federal Urban Driving Schedule (FTPR, 1996)*

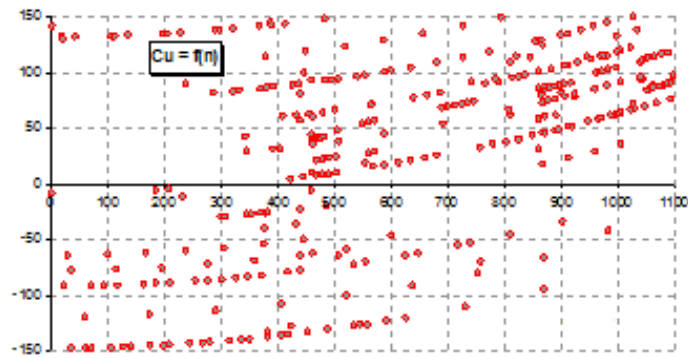*Figure 3. Instant point's _ mechanical power (FUDS Cycle)*

Figure 4. Instant point's_mechanical torque (FUDS Cycle)

2.2. Parameters constraints

In order to be integrated in a small-sized vehicle, the geometrical dimensions of the motorization are highly constrained (see Table 2). In order to meet this constraint, a literature review was carried out. (Jabbar *et al.,* 2001; Aydin *et al.,* 2006; Cho *et al.,* 2006; Parviainen, 2005; Qu *et al.*, 2006; Cavagnino *et al.,* 2002), the authors assume that the AFPMM must be more efficient than a conventional RFPMM in terms of specific power and torques. More precisely, the electromagnetic constraints are shown in Table 3.

Table 2. Geometric constraints of one electric machine

Designations	Constraints
Outside diameter (mm)	< 230
External length (mm)	< 150
External Volume (L)	< 5,5
Mass of the machine (kg)	< 13

Table 3. Electromagnetic constraints of one electric machine

Designations	Constraints
Iron losses (W)	≤ 5‰ P. mechanical for rated speed
Joule losses (W)	≤ 3% P. mechanical for rated speed
Electromagnetic torque (Nm)	> 70
Nominal efficiency (%)	> 95

3. Choice of the AFPMM

First of all, the AFPMM design involves choosing the right architecture. Several structures were identified in 2004 (Aydin *et al.*, 2004). Unfortunately, none of these structures can be used to design an axial flux motorization with respect to the following required items:

– a stator and a rotor with a minimized volume of iron (see Table 3);

– a stator windings using pre-wired coil.

With these two previous selection criteria, the state of the art revealed news and varied structures.

Marignetti *et al.* (2006) sets out a structure with a single rotor, a single stator and a single layer winding using coils wound around the teeth in order to reduce the cogging torque. Coles *et al.*, 2004; Kurronen, 2003) (see Figure 5) and Hwang *et al.* (2009) (see Figure 6), used machines with an internal stator to reduce the torque ripple and has proven the benefit in terms of power/weight of this structure.

The best motorizations of structures are presented by (Jung *et al.*, 2008) (see Figure 8) and (Hosseini *et al.,* 2011) (see Figure 7). These electric machines can meet our specifications. Indeed, the rotors are designed in a non-magnetic composite material and the stators are composed of simple magnetic circuits, having a "U" shape supporting the winding.

The ultimate choice is therefore focused on a physical structure based on some of the ideas developed in these two latest papers but while improving several structural characteristics to the rotor and the stator. (cf. Section 4.1)

The stator and the rotor of the considered AFPMM are respectively shown in Figure 9 and 10.
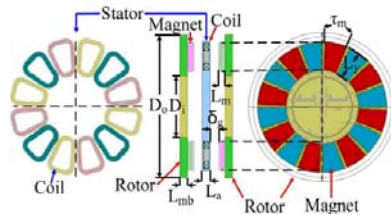

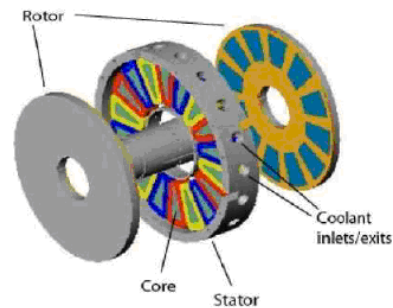Figure 5. Motor: 1 stator and 2 rotors (Kurronen, 2003)

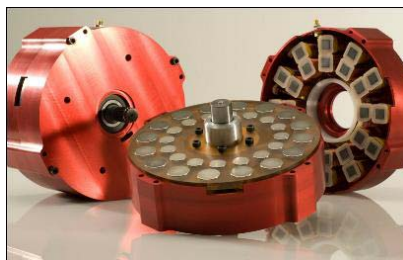Figure 6. Generator: 1 stator and 2 rotors (Hwang et al., 2009)

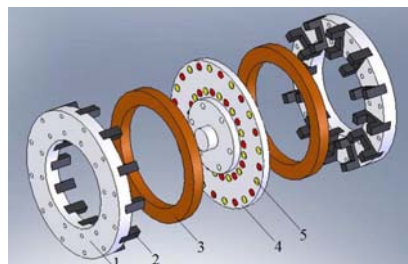Figure 7. Axial flux discoid motor (Hosseini et al., 2011)

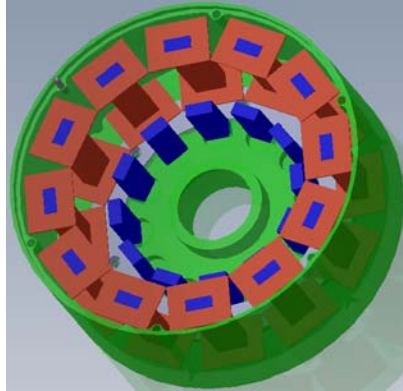Figure 8. Axial flux discoid generator (Jung et al., 2008)
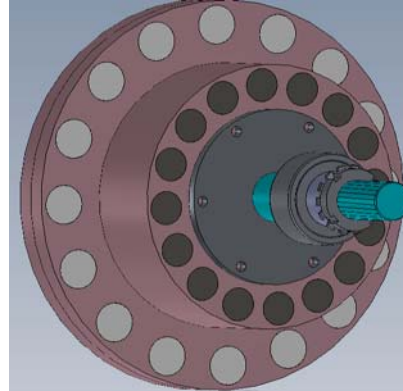
Figure 9. Half stator yoke

Figure 10. Rotor in composite structure
with magnetic bar and circular PMs

4. Presentation of the AFPMM

The overall structure of the electric motor combines the effects of variable reluctance rotor (with PMs) and electrical current supply. The magnetic circuit of the stator is designed to minimize (minimum circulation of magnetic flux lines) the ampere-turns.

4.1. Rotor design

The motorizations which are described in the articles of (Jung *et al.,* 2008) (see Figure 8) and (Hosseini *et al.*, 2011) (see Figure 7) have the particularity of having the magnetic arms of the stator in form of "U" are the same length to insert the identical coils.

This choice imposes that the rotor is flat and thin. It is likely that mechanical vibrations exist for large values of the electromagnetic torque. The mechanical vibrations are due magnetic pressure differences when the PMs of the rotor moves in front of the stator.

To solve this delicate point, in the new motorization (see Figure 10), the rotor was designed in an offset manner, with a stepped shape and in composite structure (Poirot, 2010). It also has the advantage to minimize the flux between the PMs set on the same rotor radius.

4.2. Stator design

The stator (see Figure 9) is composed of two half yokes. Each half yoke includes 12 "U" ferromagnetic. Each "U" ferromagnetic is magnetically decoupled from the

other "U". This mechanical structure will enable to decrease:

  – the risk of short-circuits between two consecutive coils;
  – the flux leakages between internal and external PMs of the rotor.

4.3. Yokes and stator arches

Inside a half stator-yoke (see Figure 11), each ferromagnetic circuit is laminated. Each "U" is held by a metallic hooping at the bottom of the stator yoke. An electric phase is composed of 8 coils wired in series, *i.e.,* 4 per half stator yoke. The distribution of the phases in each half stator yoke is performed cyclically.
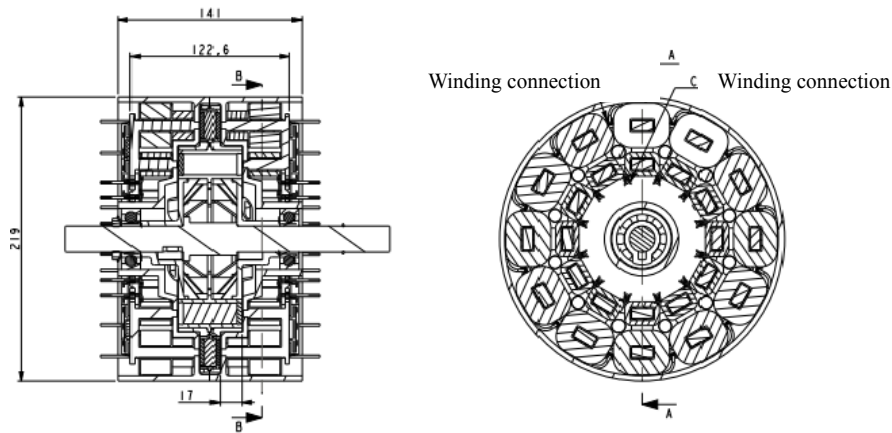

Figure 11. Axial section of the AFPMM

4.4. Operation of the AFPMM

This machine operates the same as a hybrid variable reluctance machine excited by PMs. The number of rotor poles is different from the number of stator poles. The stator coils are supplied with a system of three-phase voltages. The magnetic field created rotates at the speed Ω_s.

$$\Omega_s = \frac{\omega}{p} \tag{1}$$

where ω is the electric pulse of the currents and   the number of pole pairs in the stator.
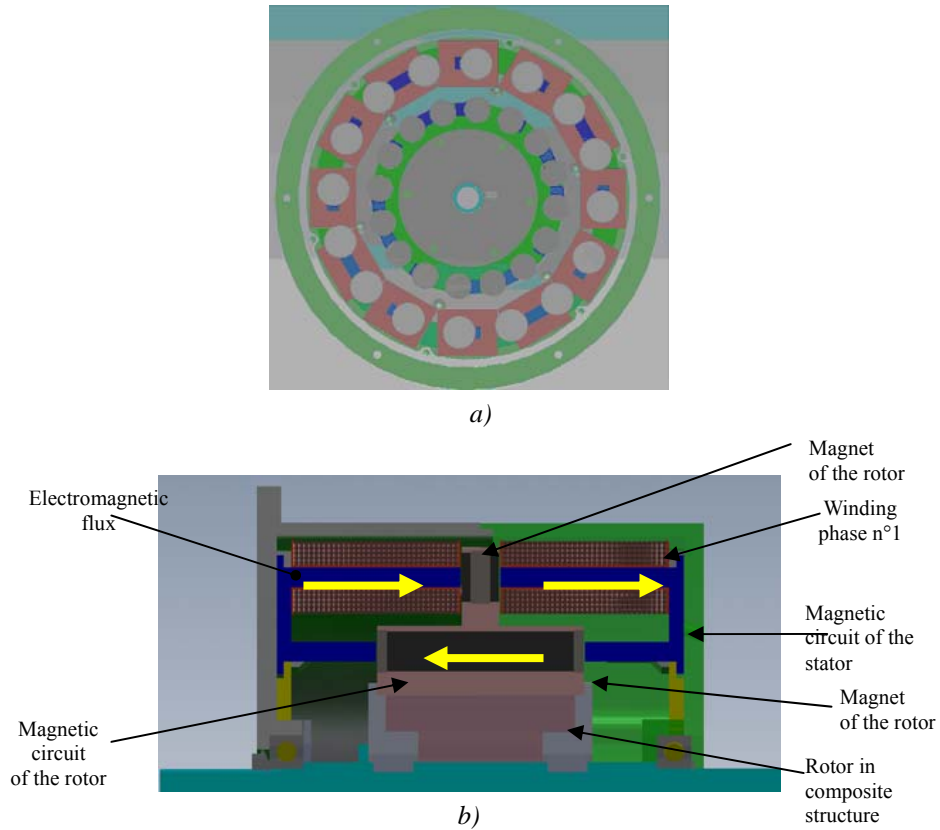
a)

b)

Figure 12. a) Radial section of the rotor and stator; b) Axial section of the rotor and stator

This new machine can operate (see Figure 12a) if the two magnetic fields (rotor and stator) have the same periodicity. The spatial period of the rotor field is:

$$p_{sr} = \frac{2\pi}{|P_r - P_s|} \tag{2}$$

The spatial period of the stator field is:

$$p_s = \frac{2\pi}{p} \tag{3}$$

Therefore, the operating condition of the AFPMM requires that the number of stator pole pairs is calculated by:

$$p = \left| P_r - P_s \right| \tag{4}$$

When the rotor rotates $4\pi \big/ P_r$ mechanical degrees (mechanical angle between a north PM and a south PM), the magnetic field of the rotor rotates a complete electrical period. Ω is the rotational speed of the rotor, P_r is the spatial period of the rotor, P_s is he spatial period of the stator. Thus, the frequency f of the mains power supply of the motorization is:

$$f = \frac{P_r \cdot \Omega}{4\pi} \tag{5}$$

The Link between Ω and ω is:

$$\Omega = \frac{2 \cdot \omega}{P_r} \tag{6}$$

In conclusion, there are two different values of P_r (Hadjidj, 1999):

$$P_r = (m-1) \cdot p \ \text{ or } \ P_r = (m+1) \cdot p \tag{7}$$

where m is the number of electrical phases of the motorization

5. 3-D FEA of the AFPMM

As the 3-D analytical modeling of this motorization would be very complex, it seemed important, as a first step, to develop a 3-D FEA accurately reproducing the electromagnetic operation of the electrical machine. The results of this model have allowed:

– the access to many of the results that a physical prototype can not provide (forms and levels of the different magnetic flux density into the machine, visualization of the flux in the air-gap and the flux leakages between internal and external PMs, etc.);

– the access to an optimization procedure that is an approach with multiple and parametric FEA.

5.1. Magnetic characteristics and motorization's mesh

The nonlinear characteristic of the ferromagnetic sheet-metal (M330-35) is used to take into account the magnetic saturation within the stator and the rotor.

This allows, in particular, the correct estimation of the value of the electromagnetic torque for a level of ampere-turns imposed. Regarding the PMs, the

magnetic characteristic *B(H)* is a straight line in the working range. The value of the PM magnetic flux density is changed according to the value of the average temperature of the PM during the various simulations. But this requires estimating the internal operating temperature of the motorization before the simulation.

As regards meshing of the geometry (see Figure 13), this must be fine enough to obtain accuracy, but must not be too dense in order not to slow down strongly the calculation time. For example, the computation time in the configuration of the Figure 13 is 30 min with a computer that has a 2.8 GHz processor.

Ultimately, it was decided that the stator and the rotor will be meshed coarsely and that the air-gap will be meshed finely. To automate the mesh a maximum element size of 2 mm is imposed at stator and rotor. As regards the air-gap the maximum element size is equal to the value of the air-gap divided by 2.
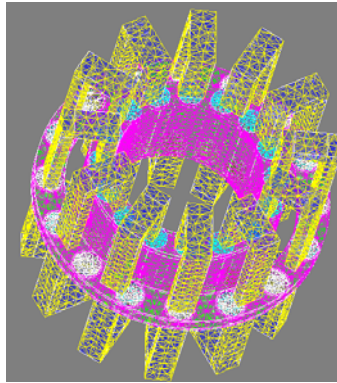

Figure 13. Mesh of the AFPMM

5.2. Electromagnetic simulations

The objective is to obtain the value of magnetic flux density at the important locations of the machine (*i.e*., air-gap, rotor, and stator arch), flux under a pole, the back EMF, etc. The plot of the equiflux lines allows one to visualize the flux passage in the entire machine and thereby to detect any flux leakages.

5.2.1. Simulations without mechanical load

5.2.1.1. Electromagnetic flux density

As regards magnetic flux density, a single magnetostatic simulation without mechanical load is useful (see Figure 14). A detailed mapping of magnetic flux density of the machine in the form of a color gradient is plotted. It is also possible to perceive the local saturation of the magnetic circuit. The most unfavorable case is

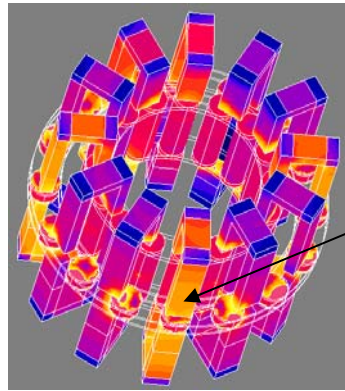when the magnetic circuit is in front of a PM (see Figure 15).

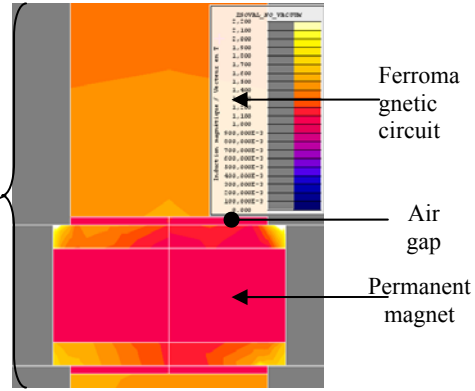*Figure 14. Magnetic flux density in the ferromagnetic circuit*

Ferromagnetic circuit

Air gap

Permanent magnet

Figure 15. Magnetic flux density in a PM

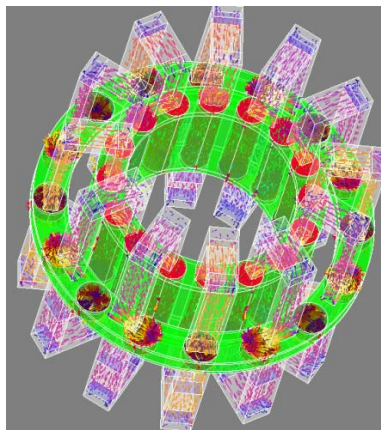*Figure 16. Visualization of the flux path*

5.2.1.2. Equiflux lines

Through the course of the arrows representing the magnetic flux (see Figure 16), it is possible to detect the magnetic leakage in the motorization. At first glance, the major leaks are around the PMs and the air-gap during rotation of the rotor. Figure 16 also shows that each magnetic circuit is independent of the others and that their own flow circulates inside properly.

The flux lines present between the PMs and between the ferromagnetic circuits are studied independently. This specific study will identify their possible impacts on the electrical performances of the electrical machine (*i.e.* the back EMF values, leakage inductances values and/or mutual inductances values).

5.2.2. Simulations with mechanical load

5.2.2.1. Electromagnetic torque

For each ampere-turns value in the stator windings a rotating speed of the rotor is imposed. The maximum value of ampere-turns was estimated *via* a thermal model (Mignot *et al.,* 2013) and corresponds to the maximum temperature value that can withstand the PMs (180°C).

5.2.2.2. PMs and stator flux in opposition

The magnetic behavior of a PM (demagnetization) is studied by measuring the value of magnetic flux density on its surface. The simulation is carried out for:

– the maximum value of the temperature of the magnet (manufacturer data) in order to take a safety margin. In this case the limit operating temperature is T_a=180°C;

– a current intensity value which should allow getting twice the rated torque.

6. Presentation of the RFPMM

The selection of the RFPMM (see Figure 17) involves choosing, first, the configuration of the rotor (Hwang *et al.,* 2010) and, second, the realization of the stator winding (Saint Michel, 2007).

Complying with the stated parameters (i.e., number of poles between the stator and the rotor, placement of the magnets in the rotor, the characteristic of the winding, etc.) the final choice was to use a motorization having the following parameters:

– the rotor is not inverted;

– the PMs are of high magnetic energy and they are placed on the surface of the rotor;

– the winding is concentric around each tooth.

This choice corresponds to several technical and economic criteria of the tender specifications.

(Jabbar *et al.,* 2001; Aydin *et al.,* 2006; Cho *et al.,* 2006; Parviainen, 2005; Qu *et al.,* 2006; Cavagnino *et al.,* 2002) confirm that, currently, this motorization is frequently used as a reference in order to compare it to new electric motors.
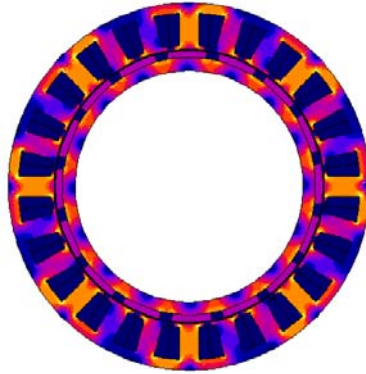
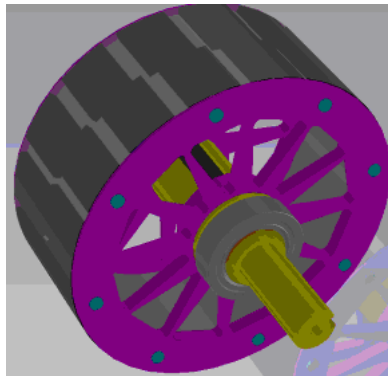*Figure 17. Radial section of the RFPMM*

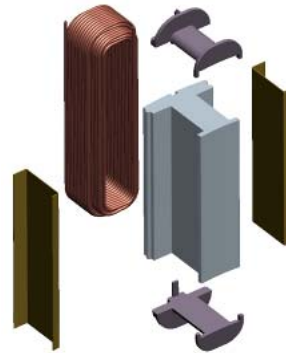*Figure 18. The rotor and the shifted PMs*   *Figure 19. Presentation the insulation of the stator teeth*

6.1. Machine geometry

6.1.1. Rotor design

Choosing to position the PMs on the surface of the rotor allows conceiving a rotor with a reduced process time. The number of poles per phase for the stator is identical to the rotor one. This solution has the advantage of using a low supply frequency, limiting the magnetic losses in the stator, but involves, on the other hand a large cogging torque as well as losses in the magnets.

The reduction of these last two points is performed by dividing into two the PMs length and by shifting them to a pre-calculated electrical angle. This will have, in addition, the advantage of obtaining a back EMF closer to a sine wave (see Figure 18 and 21).

6.1.2. Stator design

The choice of a concentrated coil around each tooth of the stator allows obtaining of a filling coefficient (in the notches) that is greater than 50 % (see Figure 19). Indeed, having small winding heads favors:

– reducing the overall volume of the machine;

– lower copper losses.

6.2. 2-D FEA of the RFPMM

6.2.1. Simulations without mechanical load

Figure 20 indicates the equiflux lines and different zones of magnetic flux density in the motorization. The value of the level of magnetic flux density in the stator is viewed in the middle: 1) at the bottom of the tooth (2,1T), 2) in the tooth (1,85T), 3) in the stator yoke (2T).
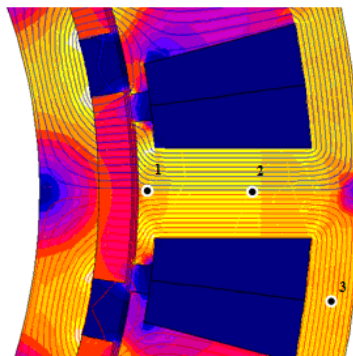

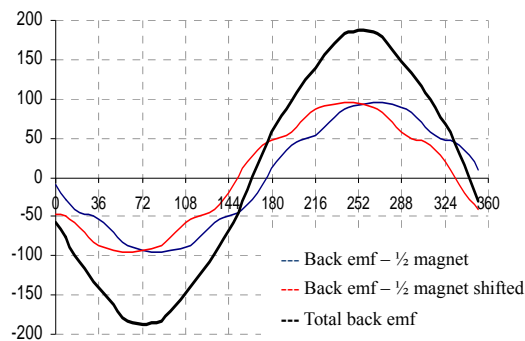*Figure 20. Visualization of tests points*

*Figure 21. Sinusoidal back EMF was obtained
by adding together the two half-back EMF*

Figure 21 shows the form of the back EMF obtained when operating without mechanical load and when the motorization functions as a generator. The optimal offset to obtain a sinusoidal back EMF was obtained by summing the two half-back EMF produced by each half-PM on the length of the rotor.

6.2.2. Simulations with mechanical load

The value and form of the electromagnetic torque were found when the motorization operates with mechanical load and for a PM temperature of 180 °C.

7. Comparison of two motorizations optimized by multiple and parametric FEA simulations

So that the comparison between the two motorizations be as consistent as possible, hereafter a reminder of the constraints that have been imposed from the beginning of the project:

   – meet the specifications described in Paragraph 2;

   – have the same number of rotor poles;

   – have the same characteristic of PM.

Taking into account the above constraints, the optimization variables for which the authors have focused for each motorization are the following:

   – the geometry and the thickness of the magnetic circuit (stator/rotor), PMs and air-gap;

   – the filling coefficient of the stator.

Tables 4 to 6 respectively provide the geometrical and electromagnetic characteristics of each machine as well as deviations between each result.

Table 4. Geometric characteristics of motorizations after optimization

Designations	RFPMM	AFPMM	Relative error (%)
Outside diameter (mm)	230	219	**-4,3**
External length (mm)	132	141	**+6,8**
External volume (L)	5,5	4,64	**-15,6**
Air-gap (mm)	2 × 0,6	4 × 0,3	/

Table 5. Electromagnetic characteristics of motorizations after optimization

Designations	RFPMM	AFPMM	Relative error (%)
PMs (T)	1,22	1,22	/
T_{orque}(Nm)	73	75	**+2,7**
$K_i(\mathrm{Nm \cdot A^{-1}})$	1,14	1,17	**+2,7**
Ferromagnetic losses (W)	120	80	**- 33**
Efficiency (%)	93	93	/

Table 6. Masses of the various active parts of both machines after optimization

Designations	RFPMM	AFPMM	Relative error (%)
Mass PMs (g)	670	300	**- 55**
Mass stator and rotor laminations (kg)	5,94	3,3	**- 46,1**
Mass of copper (kg)	2,5	2,57	**+2,8**
Mass of inactive parts (kg)	3,84	6,83	**+56**
Mass of the machine (kg)	13	13	/

7.1. Geometric and electromagnetic parameters of each motorization

The AFPMM, thanks to its special geometry, can deliver the desired torque with less external volume and ferromagnetic losses. However the thickness of the air-gap of the AFPMM must be imposed to 0.3 mm value.

7.2. Mass parameters of each motorization

With a gain of 55 % of the mass's value of the PMs and with a gain of 46 % of the overall mass's value of the stator and rotor laminations, AFPMM should represent a lower financial cost when it comes to manufacturing compared to the reference motorization. But, at the same time, despite significant gains in the mass of active parts, its overall mass is not smaller than the RFPMM.

The analysis of all masses constituting the AFPMM indicates that it is the mass of the rotor which happens to be the most restrictive. As such, it would be interesting

to investigate whether other materials could replace conventional composite structures. In conjunction with this fundamental research, it would be useful to undertake a thorough study of the mechanical forces that are applied to the rotor. These results might allow a reduction of the rotor thickness, and thus lead to a reduction of the overall mass of the machine and possibly a reduction in its axial length.

With these last two points; Motor 2 will remain as competitive as Motor 1 while being shorter and less heavy.

8. Conclusion

Comparing these two motorizations, for the same technical specifications, the results show that the AFPMM rivals this radial flux motor. Indeed, this new axial flux motorization, relative to the RFPMM, develops a superior electromagnetic torque at the same base speed, with 21% less current.

In this research work, the comparative study indicates that the performance and industrial potential of the AFPMM is of considerable interest. The study on the rotor structure, its size and the heating of the stator probably deserves particular interest to optimize its design and allow maximum simplification of its implementation.

Bibliography

Aydin M. Khambadkone A.M., Liu Qinghua (2006). Torque Quality and Comparison of Internal and External Rotor Axial Flux Surface-Magnet Disc Machines. *IEEE Transactions on Industrial Electronics*.

Aydin M., Huang S., Lipo T.A. (2004). Axial Flux Permanent Magnet Disc machines; A Review. *SPEEDAM*.

Cavagnino R., Lazzari M., Profumo F., Tenconi A. (2002). A comparison between the axial flux and the radial flux structures for PM synchronous motors, *IEEE Transactions on Magnetics.*

Cho H-W., Chungnam N., Seok-Myeong J., Sang-Kyu C. (2006). A Design Approach to Reduce Rotor Losses in High-Speed Permanent Magnet Machine for Turbo-Compressor. *IEEE Transactions on Magnetics.*

Coles P.C. (2004). Design and Analysis of an Axial Flux Permanent Magnet Machine, *IEE Conference on Power Electronics, Machines and Drives*, vol. 2, March/April, p. 840-843,

FTPR (1996). Federal Test Procedure Revisions, http://www.epa.gov/otaq/sftp.htm#cycles

Hadjidj D. (1999). *Conception, optimisation et validation d'un moteur à arceaux hybride à flux transverse,* Thèse de doctorat, Université de Franche-Comté, octobre.

Hwang K. (2010). Investigation of Torque and Iron Loss Characteristics of Optimized Spoke type IPMSM Considering Motor Modeling and Motor Drive Circuit, *IEE Proc. Elect. Power Appl.*

Hosseini S., Moghani J.S., Ershad N.F. (2011). Design, Prototyping, and Analysis of a Novel Modular Permanent-Magnet Transverse Flux Disk Generator, *IEEE Transactions on Magnetics.*

Hwang C-C., Ping-Lun L., Chuang F.C., Cheng-Tsung L. (2009). Optimization for Reduction of Torque Ripple in an Axial Flux Permanent Magnet Machine, *IEEE Transactions on Magnetics*.

Jabbar M.A. *et al.* (2001). Design and Analysis of Exterior and Interior Type High-Speed Permanent Magnet Motors. *Proc. Aust. University Power Electronics Conference.*

Jung Y-B., Long T., Nelson J., Landon C. (2008). Unique Axial Flux Motor Design Delivers Superior Torque Density. *EET-2008 European Ele-Drive Conference International Advanced Mobility Forum* Geneva, Switzerland, March 11-13.

Kroeze Ryan C., Philip T. (201l). *Electrical Battery Model for Use in Dynamic Electric Vehicle Simulations*. Illinois University.

Kurronen P. (2003). *Torque Vibration Model of Axial-Flux Surface Mounted Permanent Magnet Synchronous Machine*, Thèse de Doctorat de l'Université de Lappeenranta.

Marignetti F., Giovanni T., Cancelliere P., Delli Colli V. (2006). Electromagnetic and Mechanical design of a Fractional-slot-windings Axial-flux PM synchronous machine with Soft Magnetic Compound Stator, *IAS.*

Mignot R-B., Espanet C., Dubas F., Chamagne D. (2013). Design of an Axial Flux PM Motor using Magnetic and Thermal Equivalent Network. *Eur. Phys. J. Appl. Phys. (EPJAP)*, vol. 63, n° 3, 1-14 September.

NRCQL (2002) Norme Régissant la Catégorie des Quadricycles Lourds, "Réglementation d'ordre général : 1997 24 CE et 2002 24 CE_Réglementation sur le Couple et la

puissance : 2002-41 CE _ Réglementation sur les masses et dimensions : 1993 93 CE. http://ec.europa.eu/enterprise/sectors/automotive/documents/directives/directive-2002-24-ec_en.htm

Parviainen A. (2005). Performance comparison between low speed axial-flux and radial-flux permanent magnet machine including mechanical constraints. *IEEE Transactions on Magnetics.*

Poirot M. (2010). Enhanced Thermal Conductivity of an Epoxy-Matrix Composite Using AlN and BN fillers, ECNP Pragues.

Qu R., Aydin M., Lipo T.A. (2006). Performance comparison of dual-rotor Radial-flux and axial-flux permanent-magnet BLDC machines, *IEEE Transactions on Magnetics*.

Saint Michel J. (2007). *Bobinage des machines tournantes*, édition Techniques de l'ingénieur.

U.S_EPA (2010). Environmental Protection Agency, http://www.epa.gov/nvfel/testing/dynamometer. Htm

Wurtz F. (2005). Statut et nature des processus de conception que nous utilisons en électrotechnique et possible rationalisation et automatisation. *EF 2005*, Grenoble.